The 2009 IEEE/RSJ International Conference on
Intelligent Robots and Systems
October 11-15, 2009 St. Louis, USA

Motion Based Communication Channels between Mobile Robots – A Novel Paradigm for Low Bandwidth Information Exchange

Dhananjay Raghunathan and John Baillieul

***Abstract*—A formal notion of gesturing defined as the modulation of relative separation between mobile robots has been explored in [1]. We extend this work by developing a peer-to-peer communication channel and an associated distributed communication protocol based exclusively on the modulation of relative motion and its observation. Protocols that enable two unicycle vehicles modulating their relative separation in the plane to effectively exchange information, as well as nonlinear control laws that enable these protocols are presented. Only local information is assumed for the control action. We illustrate the contextual nature of such signaling by showing applications to secure communication as well as robot formation motion. Simulations are presented to validate the work.**

I. Introduction

Physical gestures are an important means of communication in the natural world. The use bees make of an intricate dance form to communicate information pertinent to food foraging has been widely studied [2]. It has been theorized that birds migrating in formation have a gesture based means for communicating information between each other [3]. Dragonflies are able to catch faster moving prey mid-air by modulating their motion to minimize their detection by prey[4][5]. There are several other contexts where such behavior has been documented. The underlying theme to such gesturing behavior is the existence of two or more agents that are able to *create*, *observe* and *comprehend motion*. In [1], we formalize and elucidate this notion of gesturing in the context of mobile robots.

As indicated, achieving a meaningful gesture involves at least two participants – a transmitter of the gesture and a receiver of the gesture. The transmitter needs to be able to generate motion that can be accurately perceived by the receiver. Modern day mobile robots are able to sense relative position between themselves and objects in their vicinity. A transmitter robot can exploit this fact by modulating its position relative to the receiver as a means for communication. Control strategies that help achieve such signaling as well as the notion of a *codebook* of such messages are introduced in [1][6]. [1] assumes the availability of global positioning information, and hence, the availability of a centralized infrastructure. In the present article, we extend [1] by presenting a *fully distributed strategy* to achieve such signaling.

This work was supported in the U.S. by ODDR&E MURI07 Program Grant Number FA9550-07-1-0528 and by the National Science Foundation ITR Program Grant Number DMI-0330171.

The authors are with the Mechanical Engineering Department at Boston University, Boston MA, USA.({rdjay, johnb}@bu.edu)

Prior research includes the development of control laws that enable Dubins vehicles to track a reference frame moving with constant speed and angular velocity. In [7], the authors develop a tracking control law based on a global coordinate frame of reference. The same global coordinate frame of reference is used in [8] to illustrate backstepping control design. Such strategies require centralized information from a global positioning system. In [9], the tracking problem is formulated using a local coordinate frame of reference, making the developed control laws depend only on locally observable information. Such a formulation yields a distributed rather than centralized solution to the tracking problem, and we adopt this coordinate system for this article. There is also considerable interest in the information required to maintain formation motion between robots (for instance, [10][11]), and control laws for maintaining formations in general (for instance, [12] [13].) *The information in these cases exists in the motion of the agents, but is not communicated explicitly through the motion of the agent; this is the distinguishing feature of our work.*

The article is organized as follows. We first formulate the problem as the relative motion between two unicycle vehicles constrained to move in the plane. A robot centric coordinate frame based on [9] is setup. Next, three different relative motion paradigms are discussed in sections III, IV and V. In section VI, we discuss the *contextual* nature of such signaling, and illustrate applications that use motion based signaling as a *digital data channel*. We present simulations validating our work, and conclude with open research questions.

II. Problem Formulation

As has been mentioned, our goal is to enable two agents constrained to move in the plane to convey information from one to another by modulating their relative separation. Figure 1 shows two unicycle vehicles constrained to move in the plane. In the figure, ρ represents the relative separation between the vehicles, ϕ and α represent the angles as indicated. ϕ and ρ are measured relative to the robot, while $\alpha = \theta_1 - \theta_2$ is the relative heading angle between the robots. The equations of motion are (1)-(4) (see [9].) As shown in the figure, the states are (ρ, ϕ, α). R_1 represents a receiver of information while R_2 is the transmitter of information. We represent the velocity and angular velocity of R_1 as (v_r, ω_r), and the corresponding controls for R_2 as (v, ω).

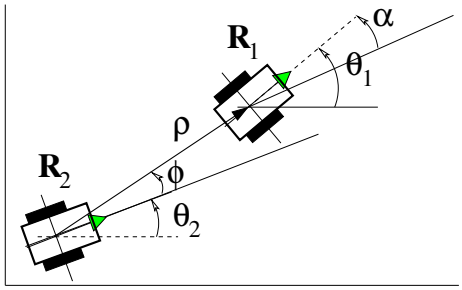

Fig. 1. Relative coordinate system between robots R_2 and R_1. $\alpha = \theta_1 - \theta_2$, where θ_1 and θ_2 are measured with respect to the inertial reference frame shown.

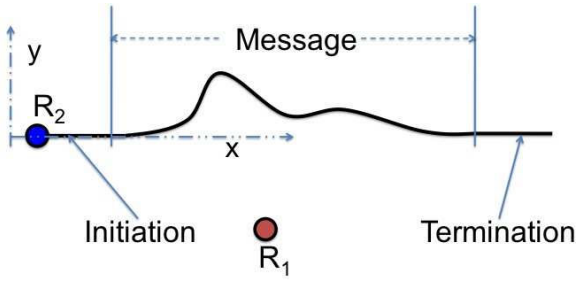

Fig. 2. Robot R_2 signaling to stationary robot R_1. Different phases of the protocol are shown. The xy-coordinate system is global, but arbitrarily selected by the robot. The receiver R_1 observes the received signal registers it.

$$\dot{\rho} = -v\cos\phi + v_r\cos(\phi - \alpha) \quad (1)$$

$$\dot{\phi} = -\omega + \frac{v\sin\phi - v_r\sin(\phi-\alpha)}{\rho} \quad (2)$$

$$\dot{\alpha} = \omega_r - \omega \quad (3)$$

$$v_r > 0 \quad (4)$$

The goal is to design control laws $\{(v,\omega),(v_r,\omega_r)\}$ so that an observation, over time, of R_2's motion conveys information to R_1. R_2's trajectory thus serves as a *message* to R_1.

It is possible for R_2 transmit a message to R_1 *independent* of R_1's motion. For this, R_2 simply tracks a planar curve that R_1 observes. The control law pairs (v,ω) and (v_r,ω_r) are thus decoupled from each other. Clearly, R_1 needs to observe the motion of R_2 *as well as* record its own motion during R_2's transmission. From this information, R_1 needs to process out R_2's motion in the plane. Such a transmission presents several practical difficulties. Sensors tend to have finite ranges for operation, and R_2 needs to move within a favorable sensory range of R_1 for R_1 to faithfully observe R_2. Secondly, complex motion on the part of R_1 implies considerable signal processing effort on its part to decipher R_2's trajectory, and possibly increase the uncertainty in the determination of R_2's trajectory.

As an alternative, it is possible for R_2 and R_1 to *cooperate* in the transmission of the message. For instance, R_1 can maintain a constant velocity trajectory along a straightline (or even a circular path), while R_2 signals information relative to this *known* trajectory. A *cooperative* strategy can alleviate the problems inherent to an *independent motion strategy*. In this article, we present a communication protocol and a sequence of control laws to achieve relative motion based message transmission in a *fully distributed* and *cooperative* fashion between two unicycle vehicles. We clarify the notion of a protocol and an associated control law by the following definitions.

Definition 1. ***Motion Based Signaling Protocol*** *A sequence of pre-determined motions that two mobile agents adopt in order to successfully exchange information.*

Definition 2. ***Signaling Control Law*** *A control law that enables mobile agents to successfully achieve a specified signaling protocol.*

We shall henceforth refer to a *motion based signaling protocol* as a *signaling protocol* for brevity. In the following sections, we discuss three *cooperative* modes of signaling information from a *transmitter* agent and a *receiver* agent.

III. Signaling information to stationary agent

We consider the case of a stationary receiver capable of sensing motion in the plane:$(v_r,\omega_r) = (0,0)$. The transmitter is a nonholonomic agent that describes a planar curve with some curvature constraints (the message.) This motion based messaging is one way: from the transmitter to the receiver. Since sensors come with a range specification, the transmitter needs to make sure that it stays within the sensing range of the sensor. Figure 2 illustrates the case when the transmitter moves in a nominally straightline trajectory and the receiver is stationary. A straight line motion of the signaling robot acts as both initiation and termination of an intervening planar curve that serves as the message. The *control objective* for the transmitter reduces to one of tracking a message curve in the plane by the signaling robot. There are several nonlinear control strategies available to achieve this, and we refer readers to [1][14] as illustrative references. There are other more complex ways of signaling to a stationary receiver (such as transmitter moving in a nominally circular trajectory) that we shall not discuss here.

IV. Signaling information between agents moving inline

In this scenario, both the transmitter and the receiver are constrained to move along a straight line in-line with each other, with $v_r > 0, \omega_r = 0$. An example of such motion includes vehicles constrained to move in traffic lanes. Figure 3 Case A illustrates this idea.

Let $x_2(0) - x_1(0) = \rho_d$, $\rho_d > 0$. Then, $\dot{x}_1 = v_1(t) = v_r \implies \dot{x}_2 = v_2(t) = v_r + A\sin(ft)$. Since we require the agents not collide, one can explicitly solve the above equations to show that $A \leq f\rho_d/2$. In addition, a bound a_{max} on the acceleration yields $\|\dot{v}_2(t)\|_\infty = \|a_2(t)\|_\infty = \|Af\cos(ft)\|_\infty \leq |Af| \implies |Af| \leq a_{max}$.

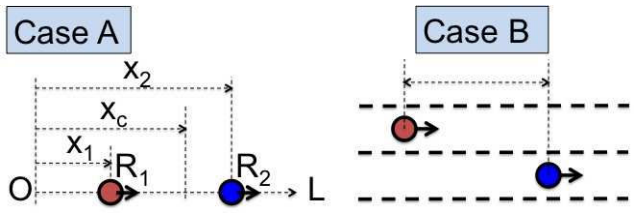

Fig. 3. Illustrates signaling between vehicles moving inline with each other. Case A shows two vehicles moving along a straight line, with R_2 signaling to R_1 by modulating the distance $x_2(t) - x_1(t)$ over time. If the two agents agree upon a common point of reference (a virtual agent) C, the the agents can signal to each other simultaneously by modulating $x_2(t) - x_c(t)$ and $x_1(t) - x_c(t)$. Case B illustrates vehicles moving in two different lanes that can signal by modulating their relative separation.

V. Signaling information between agents moving with offset but parallel nominal motions

In this section, we discuss the signaling of information between two unicycle vehicles moving in trajectories that are nominally parallel to each other. Figure 4 illustrates this mode of signaling between a transmitter agent R_2 and a receiver agent R_1. In the following subsections, we describe control laws that enable such signaling, as well as a communication protocol that the two agents need to adopt for such signaling to be feasible.

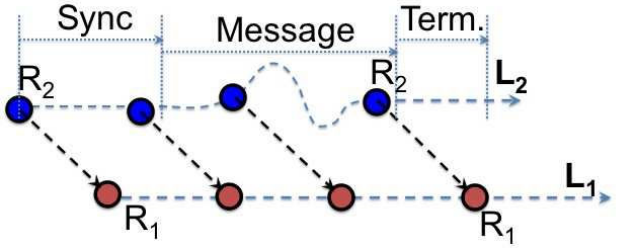

Fig. 4. R_2 is transmitting a message to R_1 through relative motion. The figure shows successive positions of R_1 and R_2 as they signal information. L_1 and L_2 represent the respective trajectories of R_1 and R_2. R_1 is moving with a constant velocity along L_1. R_2 Follows a *synchronization* (Sync) phase where it moves parallel to R_1 and offset from it by a fixed separation and orientation, as shown in the extreme left R_1-R_2 sequence. Once the two robots synchronize (i.e.the formation is stabilized), R_2 traces the message in the plane as shown, all the while keeping a constant distance and bearing with respect to R_1. Finally, it indicates the end of the message by the *termination* (Term.) phase, which is essentially a straightline trajectory.

A. Signaling Control Law

We use a technique that draws from *nonlinear feedback linearization* and *backstepping control* [15] to design a control to transmit a message to the receiver. Through algebraic manipulation, the control law (v, ω) is chosen so that the equations (1) and (2) become linear in ρ and ϕ respectively. This allows for explicit control over trajectory tracking performance with respect to ρ and ϕ, as the sequel will show. The resulting nonlinearity in equation (3) is analyzed for parameter regimes in which the states (ρ, ϕ, α) stay bounded for different signaling scenarios. For better tracking performance, two integrators γ and σ are introduced: $\dot{\gamma} = \rho - \rho_0, \dot{\sigma} = \phi - \phi_0$, where ρ_0 and ϕ_0 represent the desired orientation and bearing of R_2 relative to R_1 (Figure 1.) γ and σ represent integrators for errors in ρ and ϕ respectively. Equations (5) and (6) are the result of the outlined strategy:

$$v = \frac{v_{lin} + v_r \cos(\phi - \alpha)}{\cos\phi} \quad (5)$$

$$\omega = \omega_{lin} + \frac{v \sin\phi - v_r \sin(\phi - \alpha)}{\rho} \quad (6)$$

where

$$v_{lin} = K_{p\rho}(\rho - \rho_0) + K_{i\rho}\gamma$$
$$\omega_{lin} = K_{p\phi}(\phi - \phi_0) + K_{i\phi}\sigma$$

Equations (1)-(3), (5), (6) reduce to

$$\dot{\rho} = -K_{p\rho}(\rho - \rho_0) - K_{i\rho}\gamma \quad (7)$$

$$\dot{\phi} = -K_{p\phi}(\phi - \phi_0) - K_{i\phi}\sigma \quad (8)$$

$$\dot{\alpha} = -\omega_{lin} - v_{lin}\frac{\tan\phi}{\rho} - \frac{v_r}{\rho}\left[\tan\phi\cos(\phi - \alpha) - \sin(\phi - \alpha)\right] \quad (9)$$

$$\dot{\gamma} = \rho - \rho_0 \quad (10)$$

$$\dot{\sigma} = \phi - \phi_0 \quad (11)$$

We start by investigating the local stability of the equations (7)-(11). We note that this reduced set of equations assumes $v_r > 0$ for the formulation to be valid.

Theorem V.1. *The point* $(\rho_0, \phi_0, 0, 0, 0)$ *is an asymptotically stable equilibrium point for the system* (7)-(11) *for* $K_{p\rho} > 0, K_{p\phi} > 0, K_{i\rho} > 0, K_{i\phi} > 0, \phi_0 \in (-\pi/2, \pi/2), v_r > 0, \rho_0 > 0$.

Proof: See Appendix. ■

We next consider the performance of the system (7)-(11) to sinusoidal excitation. Theorem V.3 quantifies the tracking error and the feasible parameter ranges for this problem.

Lemma V.2. *Consider constants* $a \in \mathbb{R}^+$, $\mathbf{b} \in \mathbb{R}^n$, *a vector* $\mathbf{x} \in \mathbb{R}^n$, *and a function* $g(\cdot) : \mathbb{R}^n \to \mathbb{R}$ *defined as* $g(\mathbf{x}) = -a\|\mathbf{x}\|_2^2 + \mathbf{b}^T\mathbf{x}$. *Then,* $\|\mathbf{x}\| > \|\mathbf{b}\|/a \implies g(\mathbf{x}) < 0$.

Proof: We have $g(\mathbf{x}) \leq -a\|\mathbf{x}\|^2 + \|\mathbf{b}\|\|\mathbf{x}\| = a\left(-\|\mathbf{x}\| + \|\mathbf{b}\|/a\right)\|\mathbf{x}\|$, and hence the result. ■

Theorem V.3. *For the system* (7)-(11)*, let the reference input be of the form:*

$$\dot{s} = v_r, \quad [v_r > 0,\ \omega_r = 0,\ s(0) = 0]$$
$$\rho_0(s) = \rho_0 - \rho_s\cos(\omega_s s) \quad [0 < \rho_s < \rho_0,\ \omega_s > 0]$$
$$\phi_0(s) = \phi_0 + \tan^{-1}(\rho_s\omega_s\sin(\omega_s s))$$
$$\sup_{s\in\mathbb{R}} |\ \phi_0(s)\ | < \pi/2$$

Let the errors to this reference input be $\rho_{err}(t) = \rho(t) - \rho_0(t)$, $\phi_{err}(t) = \phi(t) - \phi_0(t)$. *For initial errors* $[\rho_{err}(0), \phi_{err}(0), \alpha(0)]$ *sufficiently close to the origin, there exist feasible choices of* $K_{p\rho}, K_{i\rho}, K_{p\phi}, K_{i\phi}$ *for which the errors* $\rho_{err}(t)$, $\phi_{err}(t)$, *and* $\alpha_{err}(t)$ *are bounded for all time.*

Proof: We analyze the solution on a state by state basis. For $\phi_{err}(t)$, we have

$$\begin{aligned}\dot{\phi}_{err} &= \dot{\phi} - \dot{\phi}_0 = -K_{p\phi}\phi_{err} - K_{i\phi}\sigma - \dot{\phi}_0 \\ &= -K_{p\phi}\phi_{err} - K_{i\phi}\sigma + \frac{\rho_s\omega_s^2 v_r\cos(\omega_s v_r t)}{1+\rho_s^2\omega_s^2\sin^2(\omega_s v_r t)} \quad (12)\end{aligned}$$

The above can be collected as the following system:

$$\begin{aligned}\begin{bmatrix}\dot{\phi}_{err}\\ \dot{\sigma}\end{bmatrix} &= \begin{bmatrix}-K_{p\phi} & -K_{i\phi}\\ 1 & 0\end{bmatrix}\begin{bmatrix}\phi_{err}\\ \sigma\end{bmatrix} + \mathbf{f}(t) \quad (13)\\ \mathbf{f}(t) &= \begin{bmatrix}\frac{\rho_s\omega_s^2 v_r\cos(\omega_s v_r t)}{1+\rho_s^2\omega_s^2\sin^2(\omega_s v_r t)}\\ 0\end{bmatrix} = \begin{bmatrix}f(t)\\ 0\end{bmatrix}\end{aligned}$$

We consider a Lyapunov function $V = \mathbf{x}^T\mathbf{P}\mathbf{x}$ where $\mathbf{x} = [\phi_{err}, \sigma]^T$, and $\mathbf{P} > 0$. Let $\mathbf{A} = [-K_{p\phi}, K_{i\phi}; 1, 0]$. We have, for the nominal system $\dot{\mathbf{x}} = \mathbf{A}\mathbf{x}$, $\dot{V} = \mathbf{x}^T(\mathbf{A}^T\mathbf{P} + \mathbf{P}\mathbf{A})\mathbf{x} < 0$ if and only if there exists some $\mathbf{Q} > 0$ such that $\mathbf{A}^T\mathbf{P} + \mathbf{P}\mathbf{A} = -\mathbf{Q}$. For $\mathbf{Q} = [1, 0; 0, 1]$, $K_{p\phi}, K_{i\phi} > 0$, it is not hard to show that

$$\mathbf{P} = \begin{pmatrix}\frac{1+K_{i\phi}}{2K_{i\phi}K_{p\phi}} & \frac{1}{2K_{i\phi}}\\ \frac{1}{2K_{i\phi}} & \frac{K_{i\phi}+K_{i\phi}^2+K_{p\phi}^2}{2K_{i\phi}K_{p\phi}}\end{pmatrix}$$

For the system (13), the Lyapunov function becomes

$$\begin{aligned}\dot{V} &= -\|\mathbf{x}\|_2^2 + 2f(t)\left(-\frac{-1-K_{i\phi}}{2K_{i\phi}K_{p\phi}}\phi_{err} + \frac{1}{2K_{i\phi}}\sigma\right)\\ &\leq -\|\mathbf{x}\|_2^2 + 2f(t)\frac{\sqrt{(1+K_{i\phi})^2+K_{p\phi}^2}}{2K_{i\phi}K_{p\phi}}\|\mathbf{x}\|_2\end{aligned}$$

We observe that $\sup_t f(t) = \rho_s\omega_s^2 v_r$. Lemma V.2 implies

$$\dot{V} < 0 \iff \|\mathbf{x}\|_2 > \rho_s\omega_s^2 v_r\frac{\sqrt{(1+K_{i\phi})^2+K_{p\phi}^2}}{K_{i\phi}K_{p\phi}} \quad (14)$$

Thus $\|[\phi_{err}, \sigma]\|_2 < +\infty$ and hence, $\phi_{err}(t)$ is bounded.
Equation (14) implies that all trajectories starting inside $\|\mathbf{x}\|_2 > \rho_s\omega_s^2 v_r\sqrt{(1+K_{i\phi})^2+K_{p\phi}^2}/(K_{i\phi}K_{p\phi}) + \epsilon_\omega,\ \epsilon_\omega > 0$ have $\dot{V} < 0$, and hence, do not leave this region. Equation (14) serves as an estimate of the bound on the error.
A similar argument can be made to prove boundedness of $\rho_{err}(t)$. For $\rho_{err}(t)$, we have

$$\begin{aligned}\dot{\rho}_{err} &= \dot{\rho} - \dot{\rho}_0 = -K_{p\rho}\rho_{err} - K_{i\rho}\gamma - \dot{\rho}_0\\ &= -K_{p\rho}\rho_{err} - K_{i\rho}\gamma + \rho_s\omega_s\sin(\omega_s v_r t) \quad (15)\end{aligned}$$

With the replacements $\phi_{err} \to \rho_{err}, \sigma \to \gamma, K_{p\phi} \to K_{p\rho}, K_{i\phi} \to K_{i\rho}, f(t) \to \rho_s\omega_s\sin(\omega_s v_r t)$ in the arguments for the boundedness of $\phi_{err}(t)$, one can find a similar bound:

$$\|[\rho_{err}, \gamma]\|_2 > \rho_s\omega_s\frac{\sqrt{(1+K_{i\rho})^2+K_{p\rho}^2}}{K_{i\rho}K_{p\rho}} \quad (16)$$

Thus all trajectories starting within $\|[\rho_{err}, \gamma]\|_2 = \rho_s\omega_s\sqrt{(1+K_{i\rho})^2+K_{p\rho}^2}/(K_{i\rho}K_{p\rho}) + \epsilon_v,\ \epsilon_v > 0$ have $\dot{V} < 0$, and hence do not leave this region.

Finally, for the state α, we have

$$\dot{\alpha} = -\omega_{lin} - \underbrace{\left(\frac{\tan\phi}{\rho}\right)}_{p(t)}v_{lin} - \underbrace{\left(\frac{v_r}{\rho\cos\phi}\right)}_{r(t)}\sin\alpha$$

We show that $\omega_{lin}, v_{lin}, p(t), q(t)$ are bounded functions. We have

$$\|\omega_{lin}\|_2 = \|K_{p\phi}\phi_{err} + K_{i\phi}\sigma\|_2 \leq \sqrt{K_{p\phi}^2+K_{i\phi}^2}\,\|[\phi_{err}, \sigma]\|_2$$

and hence, $\|\omega_{lin}\|_2$ is bounded (using (14).) Similarly, $\|v_{lin}\|_2$ is bounded. $0 < \rho(t) < +\infty$ and $0 \leq |\phi(t)| < \pi/2$ implies that (a) $p(t)$ and $r(t)$ are bounded, and (b) $r(t) > 0$.
Using the Lyapunov function $V = 2 - 2\cos^2(\alpha/2)$, we have

$$\begin{aligned}\dot{V} &= \dot{\alpha}\sin\alpha = -r(t)\sin^2\alpha + \sin\alpha(-\omega_{lin} - v_{lin}p(t))\\ &\leq -r(t)\sin^2\alpha + |\sin\alpha|\,|(-\omega_{lin} - v_{lin}p(t))|\end{aligned}$$

Using Lemma V.2, we find a $b, b \in [0, 1)$ such that

$$|\sin\alpha| > b = \sup_{t\in[0,\infty)}\left|\frac{-\omega_{lin} - v_{lin}p(t)}{r(t)}\right| \implies \dot{V} < 0 \quad (17)$$

The goal is to choose parameters that satisfy this inequality. Using a more conservative bound, we have, using $\max_t \rho\cos\phi = \rho_0 + \rho_s$, and, $|\phi| \in [0, \pi/2) \Rightarrow \max_t \sin\phi < 1$,

$$\begin{aligned}&\sup_{t\in[0,\infty)}\left|\omega_{lin}\frac{\rho\cos\phi}{v_r} + v_{lin}\frac{\sin\phi}{v_r}\right|\\ \leq\ &\sup_{t\in[0,\infty)}\left|\omega_{lin}\frac{\rho\cos\phi}{v_r}\right| + \left|v_{lin}\frac{\sin\phi}{v_r}\right| < 1\\ \Rightarrow\ &\frac{\sqrt{K_{p\phi}^2+K_{i\phi}^2}}{v_r/(\rho_0+\rho_s)}\left[\frac{\rho_s\omega_s^2 v_r\sqrt{(1+K_{i\phi})^2+K_{p\phi}^2}}{K_{i\phi}K_{p\phi}} + \epsilon_\omega\right] +\\ &\frac{\sqrt{K_{p\rho}^2+K_{i\rho}^2}}{v_r}\left[\frac{\rho_s\omega_s\sqrt{(1+K_{i\rho})^2+K_{p\rho}^2}}{K_{i\rho}K_{p\rho}} + \epsilon_v\right] < 1\end{aligned} \quad (18)$$

The above inequality yields conditions on parameters so that $\alpha(t)$ is bounded. It is possible to select $K_{p\phi}, K_{p\rho}, K_{i\phi}, K_{i\rho}$ for the range of values of $\rho_s, \omega_s > 0, v_r$ that satisfy the above inequality. Note that ϵ_ω and ϵ_v are arbitrarily small. Since each of the states $\rho_{err}(t)$, $\phi_{err}(t)$ and $\alpha(t)$ are bounded for all $t \in [0, \infty)$, the result follows. ■
We observe in (18) that for large ω_s, the gains also need to be large which can lead to saturation of the velocity/angular velocity of the vehicle. Also, it is possible to analyze $\rho_{err}(t)$ in (15) as a standard second order system with damping subject to sinusoidal excitation.
Figures 5 and 6 illustrate the performance of this control law. The plots show the evolution of the states of the plant as the system follows a fixed target and a sinusoidal trajectory respectively.

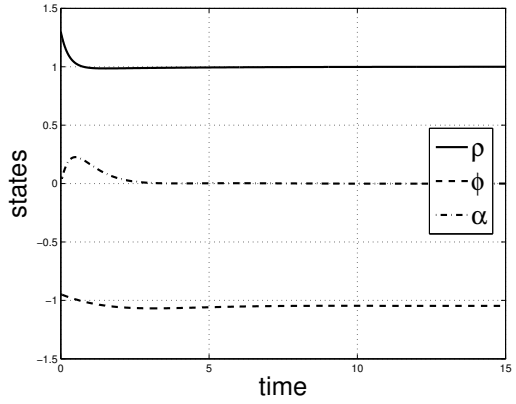

Fig. 5. Parameters are $\rho(0) = 1.3, \rho_0 = 1.0, \phi(0) = -\frac{\pi}{3} + .1, \phi_0 = -\frac{\pi}{3}, v_r = .5, K_{p\rho} = 4.0, K_{p\phi} = 1.0, K_{i\rho} = 1.0, K_{i\phi} = .5, \omega_r = 0.0$.

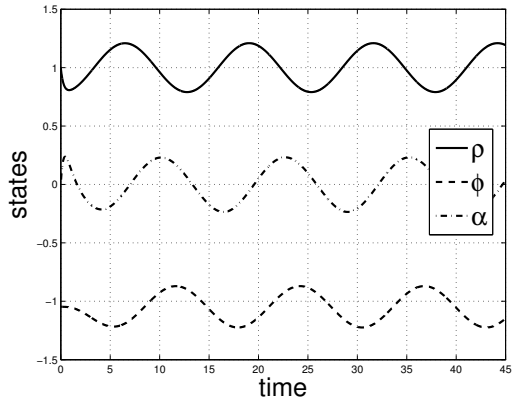

Fig. 6. Parameters are $\rho(0) = 1.0, \rho_0(s) = 1.0 - 0.2\cos(s), \phi(0) = -\pi/3, \phi_0(s) = -\pi/3 + \tan^{-1}(0.2\sin(s)), v_r = .5, K_{p\rho} = 4.0, K_{p\phi} = 1.0, K_{i\rho} = 1.0, K_{i\phi} = .5, \omega_r = 0.0$.

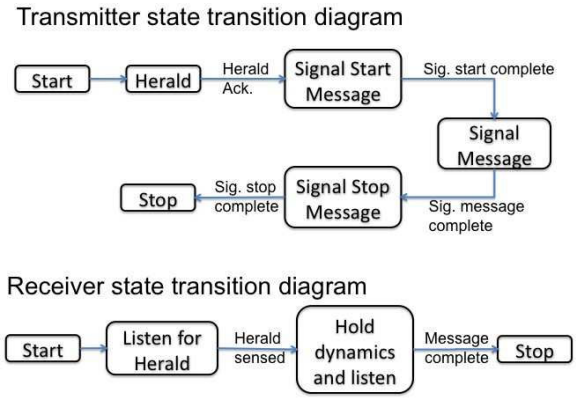

Fig. 7. State transition diagram for the transmitter and the receiver as the work in collaboration to achieve signaling of information from the transmitter to the receiver. This is a simplex transmission protocol.

B. Protocol Implementation and state transition diagrams

Figure 7 shows a protocol that a transmitter and receiver agent need to follow in order to exchange information from the transmitter to the receiver. As one can see, there is a sequence of states and events (messages) that help in the transmission of information from one robot to the other. The state transition is as follows. The receiver is in some state of motion, and the transmitter attempts to *herald* the receiver. A typical heralding motion can be that of tracking the receiver at a pre-determined separation and orientation from the receiver. Once the receiver senses the *herald* message from the transmitter, the receiver can start following trajectories that are easy to track – such as a straight line trajectory – as a *Herald Acknowledge* message. The receiver thus *cooperates* with the transmitter as part of this protocol. Once the transmitter receives a *Herald Acknowledge* message, the transmitter starts synchronizing with the receiver's motion. It maintains the fixed separation and orientation motion with respect to the receiver, and estimates any parameters that it requires (such as v_r, ω_r). This motion also serves as the *Signal Begin Message*. It then transmits its message using the control laws described in the previous section, and finally, reverts to a motion where it maintains a fixed separation and orientation with respect to the receiver (the *Signal End Message*.) Clearly this final motion needs to be time bounded.

The protocol described is a best effort protocol, and can be misinterpreted at various stages. For instance, the receiver could misinterpret the transmitter's tracking motion with intent to *herald* as hostile. Alternately, the receiver could misinterpret a hostile agents intensions as a heralding gesture. Resolving such ambiguities with maximal reliability is part of our ongoing research.

VI. The Contextual Nature of Motion-based Communication

Motion-based signaling can be used to communicate information in a variety of different contexts. In what follows, we show how a motion-based communication channel can be used for communicating signals ranging from digitally encoded information (which can be arbitrarily long) to explicit motion based messages for robot formation changes (mimicking ideas from nature such as the bee-dance[2]).

Example VI.1. ***A low bandwidth digital data stream channel*** *One can use the motion-based signaling channel for transmitting a data stream. To do this, we need an alphabet of messages that can be transmitted. Consider a codebook $\mathcal{B}$ composed of a finite number of polynomials from the set of Chebyshev polynomials of the first kind. The first five terms are $T_0(x) = 0$, $T_1(x) = x$, $T_2(x) = -1 + 2x^2$, $T_3(x) = -3x+5x^3$, $T_4(x) = 1-8x^2+8x^4$. These polynomials have the property that $\|T_i(x)\|_\infty \leq 1, x \in [-1, 1], i \in \{1, 2, 3, 4, \dots\}$. This property guarantees bounds on the minimum and maximum separation between two agents exchanging a message from this set. A finite set of these polynomials can form the alphabets for codewords in our signaling scheme (after scaling them to ensure sufficient tracking performance.) We represent by $\mathcal{B}_p^5$ the codebook formed by concatenating elements from the set $\{T_0(x), T_1(x), T_2(x), T_3(x), T_4(x)\}$, with the element*

$T_0(x)$ being reserved to indicate the start and stop of a transmission. We assume that the polynomials are scaled appropriately to meet curvature and slope bounds. Circular arcs can be used to get matching slopes at either ends of the signaled alphabet in each codeword. Figure 8 illustrates the states of a transmitter-receiver pair as a function of time as the transmitter transmits a message from $\mathcal{B}_p^5$.

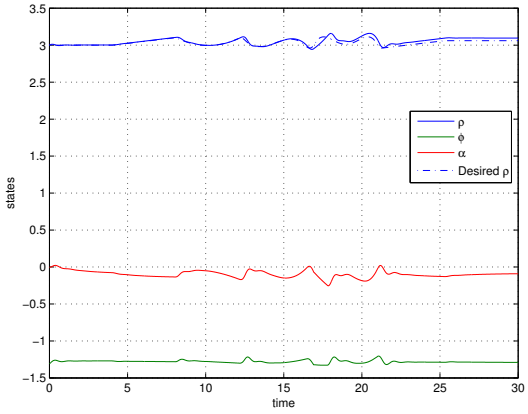

Fig. 8. The sequence $T_0, 0.05T_1, 0.05T_2, 0.05T_3, 0.05T_4, 0.05T_1, T_0$, which is an element of $\mathcal{B}_p$ is signaled.

Example VI.2. ***The Diffie-Hellman Key Agreement Scheme using relative motion*** *The Diffie-Hellman Key Agreement Scheme is widely used to generate a common encryption key for secure communication between two entities that do not have a secure communication medium (see [16] for instance.) Consider two agents Alice and Bob that wish to exchange a secret shared key that is to be used to encrypt messages that the exchange with each other. To do this, they both share a common pair (P, g), $P \in \mathbb{Z}^+, g \in \mathbb{Z}^+$ that is publicly known and satisfies (1) P is prime, (2) $1 < g < P$, (3) $\forall\ n \in \mathbb{Z}^+$ such that $1 \leq n < P$, $\exists\ k \in \mathbb{Z}^+$ such that $n = g^k \mod P$. Now, Alice and Bob each choose a positive integer K_a and K_b respectively, and compute $y_a = g^{K_a} \mod P$ and $y_b = g^{K_b} \mod P$. They then exchange y_a and y_b over an insecure channel. The common key can be computed as $K = (g^{K_a K_b} \mod P) = (y_b^{K_a} \mod P) = (y_a^{K_b} \mod P)$. Figure 9 **A** illustrates this protocol as a timeline diagram. The drawback in this key exchange scheme is shown in Figure 9 **B**. An interloper can intercept y_a and essentially impersonate Alice to Bob by using its own key K_a^*, and vice versa. The possibility of such an interloper is precluded by using relative motion signaling to exchange y_a and y_b. Once the key is established, secure wireless communication can be achieved between the agents.*

Typically, P tends to be a very large prime (to the order of 1024 bits.) A 4-element Chebyshev basis as shown in the previous example will require $1024 \log_4 2 = 512$ alphabet transmissions. Even with a transmission of one symbol every 2 seconds (which is quite fast for such vehicles), it will takes over 34 minutes to transmit such a long key! Compressing more information into a codebook or working with a shorter key that is constantly updated is the subject of ongoing research.

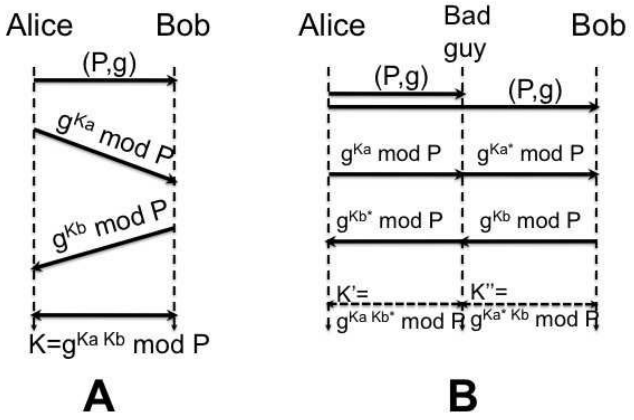

Fig. 9. **A** illustrates the Diffie-Hellman Key Sharing Scheme. **B** shows an interloper that is able to evade detection and maintain separate channel connections between Alice and Bob. This can be prevented by using a motion-based signaling scheme.

VII. Conclusions

We have shown that relative motion between nonholonomic vehicles in the plane can be used to exchange information. A distributed control law and a communication protocol have been presented to achieve such signaling has been presented, as have been some promising applications. There are open research questions that need to be resolved for successful deployment of this concept in the real world. Noisy motion (such as motion on uneven terrain) needs to be accounted for, as well as noisy observations (sensor noise). The protocol needs to be robust to obstacles in the plane, and unambiguous in interpretation. Control laws that are able to handle non-zero ω_r as well as uncertainties in (v_r, ω_r) need to be developed. Finally, such signaling need not be restricted to the plane, but could be extended to 3D (Unmanned Arial Vehicles for instance.) The information theory for such signaling needs to be investigated to determine the limits to which such a technique of communication can be stretched. These form parts of our on-going research.

Appendix
Proof of Theorem V.1

The system (7)-(11) has a fixed point (verified by substitution) $(\rho_0, \phi_0, 0, 0, 0)$ and is differentiable. Linearizing the system about this fixed point yields the Jacobian (19) (see next page.) The characteristic equation of (19) factors to $\frac{1}{\rho_0}[\,(\lambda^2 + \lambda K_{p\rho} + K_{i\rho})(\lambda^2 + \lambda K_{p\phi} + K_{i\phi})(\lambda\rho_0 + \cos\phi_0 V_r + \sin\phi_0 V_r \tan\phi_0)]$. The conditions $\phi_0 \in (-\pi/2, \pi/2), v_r > 0, \rho_0 > 0$ ensure that the elements of $\mathbf{A}$ do not diverge. The conditions $K_{p\rho} > 0, K_{p\phi} > 0, K_{i\rho} > 0, K_{i\phi} > 0$ ensure stable eigenvalues for $\mathbf{A}$ by the *Routh stability criterion* ([17]).

$$\mathbf{A} = \begin{pmatrix} -K_{\mathrm{p}\rho} & 0 & 0 & -K_{\mathrm{i}\rho} & 0 \\ 0 & -K_{\mathrm{p}\phi} & 0 & 0 & -K_{\mathrm{i}\phi} \\ \frac{-K_{\mathrm{p}\rho}\tan(\phi_0)}{\rho_0} & -K_{\mathrm{p}\phi} - v_r\frac{-\cos(\phi_0)+\sec(\phi_0)-\sin(\phi_0)\tan(\phi_0)}{\rho_0} & -\frac{V_r\sec(\phi_0)}{\rho_0} & \frac{-K_{\mathrm{i}\rho}\tan(\phi_0)}{\rho_0} & -K_{\mathrm{i}\phi} \\ 1 & 0 & 0 & 0 & 0 \\ 0 & 1 & 0 & 0 & 0 \end{pmatrix} \tag{19}$$

REFERENCES

[1] D. Raghunathan and J. Baillieul, "Exploiting information content in relative motion," Americal Control Conference, June 2009.

[2] A. Michelsen, "The transfer of information in the dance language of honeybees: progress and problems," Journal of Comparative Physiology A: Neuroethology, Sensory, Neural, and Behavioral Physiology, vol. 173, no. 2, pp. 135–141, August 1993.

[3] P. Seiler, A. Pant, and K. Hedrick, "Analysis of bird formations," in Proceedings of the 41st IEEE Conference on Decision and Control, Las Vegas, NV, December 2002.

[4] P. Glendinning, "The mathematics of motion camouflage," Proceedings of the Royal Society of London B, vol. 271, pp. 477–481, 2004.

[5] P.V.Reddy, E.W.Justh, and P.S.Krishnaprasad, "Motion camouflage in three dimensions," in Conference on Decision and Control. IEEE, December 2006, pp. 3327–3332.

[6] D. Raghunathan and J. Baillieul, "Relative motion of robots as a means for signaling," in International Conference in Industrial Automation and Robotics, ICIAR. IAENG, July 2008.

[7] Y. Kanayama, Y. Kimura, F. Miyazaki, and T. Noguchi, "A stable tracking control method for an autonomous mobile robot," Internation Conference on Robotics and Automation, vol. 1, pp. 384–389, May 1990.

[8] Z.-P. Jiang and H. Nijmeijer, "Tracking control of mobile robots: A case study in backstepping," Automatica, vol. 33, no. 7, pp. 1393–1399, 1997.

[9] J. Baillieul and A.Suri, "Information patterns and hedging brockett's theorem in controlling vehicle formations," in Proceedings of the 2003 IEEE Conference on Decision and Control, Maui, Hawaii,USA, December 2003, pp. 556–563.

[10] J. Fax and R. M.Murray, "Information flow and cooperative control of vehicle formations," IEEE Trans.on Automatic Control, vol. 49,NO.9, pp. 1465–1476, Sep. 2004.

[11] J.Baillieul and L.McCoy, "The combinatorial graph theory of structured formations," in 46th IEEE Conference on Decision and Control. New Orleans, LA, USA: IEEE, December 2007.

[12] M. Egerstedt and X. Hu, "Formation constrained multi-agent control," in International Conference on Robotics and Automation, Seoul, Korea, May 2001.

[13] H. Tanner, G. Pappas, and V. Kumar, "Leader-to-formation stability," in IEEE Transactions on Robotics and Automation, vol. 20, no. 3, June 2004, pp. 443–455.

[14] M. P and Samson.C, "Trajectory tracking for non-holonomic vehicles: overview and case study," in Proceedings of the Fourth International Workshop on Robot Motion and Control, June 2004, pp. 139–153.

[15] H. K. Khalil, Nonlinear Systems, Third, Ed. Prentice Hall, 2002.

[16] D. R. Stinson, Cryptography Theory and Practice, 3rd ed., K. H.Rosen, Ed. Chapman & Hall/CRC, 2006.

[17] N. S. Nise, Control Systems Engineering, Fourth, Ed. John Wiley & Sons, Inc., 2004.